

Supporting information

for

Doxorubicin-loaded core-shell UiO-66@SiO₂ metal-organic frameworks for targeted cellular uptake and cancer treatment

Daria B. Trushina^{1,2}, Anastasia Yu. Sapach^{2,3}, Olga Burachevskaya⁴, Pavel V. Medvedev⁴,
Dmitry N. Khmelenin¹, Tatiana N. Borodina¹, Mikhail A. Soldatov⁴, Vera V. Butova^{4*}

¹ Federal Research Center Crystallography and Photonics, Russian Academy of Sciences, Moscow 119991 Russia

² Sechenov First State Medical University, Moscow 119991 Russia

³ Skolkovo Institute of Science and Technology, Moscow 143025, Russia

⁴ The Smart Materials Research Institute, Southern Federal University, Rostov-on-Don 344090, Russia

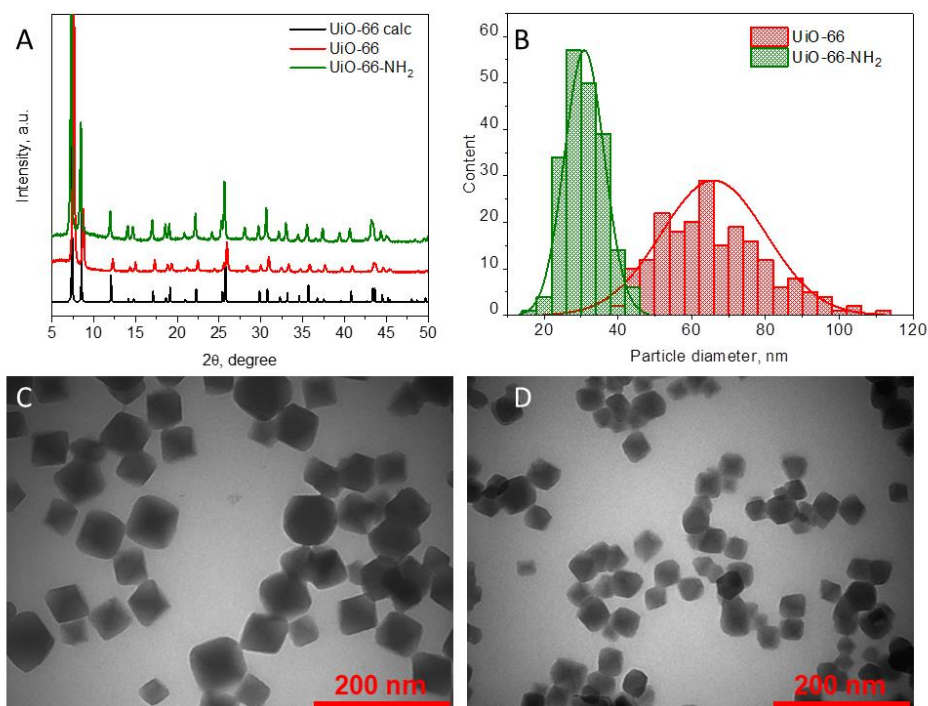


Figure S1. Powder XRD patterns of samples UiO-66 and UiO-66 NH₂ (A). Profile UiO-66 calc was calculated according to crystallographic information from 10.1021/cm1022882. Particle-sized distribution according to TEM images from 200 particles (B). Representative TEM images of UiO-66 (C) and UiO-66-NH₂ (D) samples.

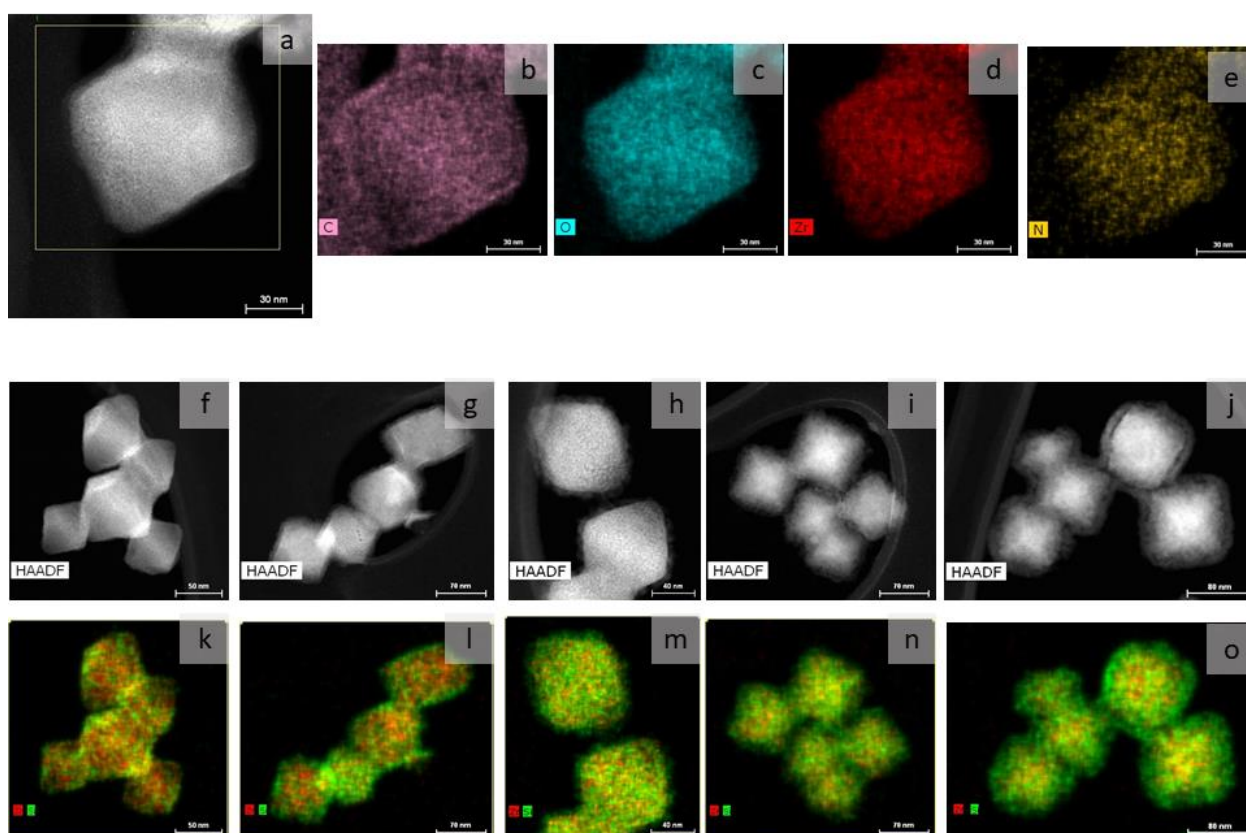


Figure S2. TEM images of UiO-66-NH₂ MOFs with maps of C, O, Zr, and N (a-e). HAADF images and corresponding Zr-Si elemental maps for UiO-66-NH₂@SiO₂ samples obtained by incubation of nanoparticles in TEOS for 0.5h (f, k), 1h (g, l), 2h (h, m), 4h (i, n), 24h (j, o).

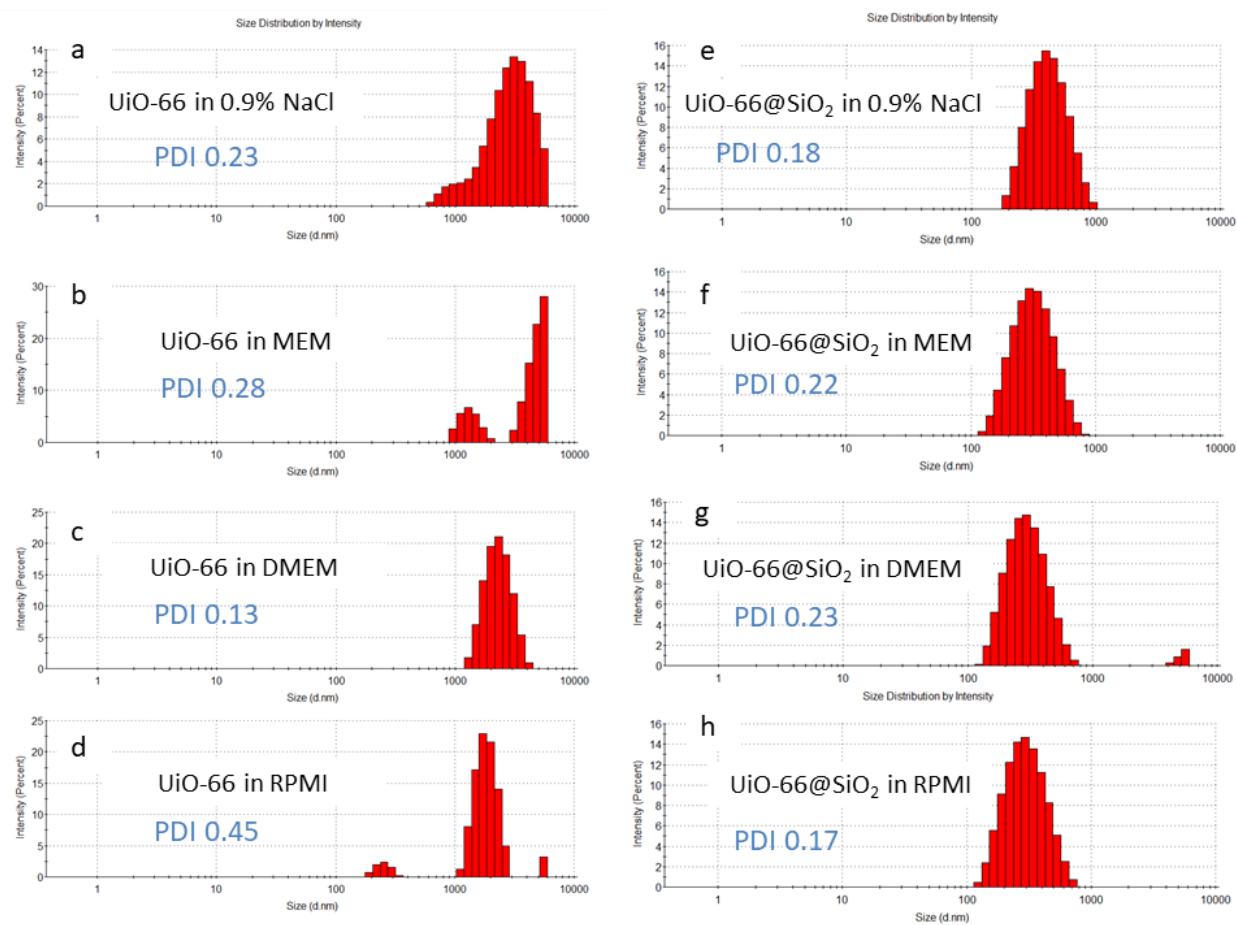


Figure S3. DLS-intensity results for UiO-66 and UiO-66@SiO₂ MOFs dispersed in saline solution, MEM, DMEM and RPMI cell culture media.

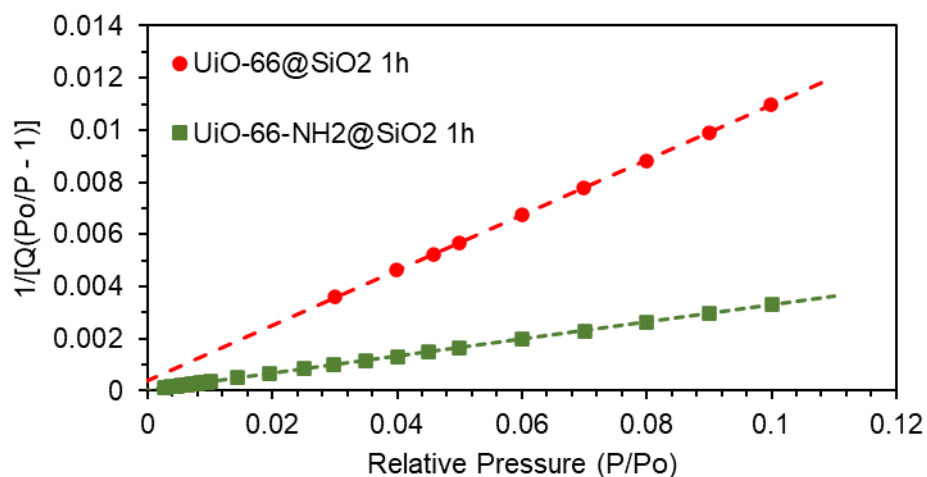


Figure S4. BET surface area plots for UiO-66@SiO₂ 1h (red) and UiO-66-NH₂@SiO₂ 1h (green) samples. Markers represent experimental data; dashed lines show BET approximation.

Table S1. Details of porosity calculations. SSA stands for specific surface area, C is the BET constant.

	BET			Total pore volume, mm ³ /g	t-plot calculations			
	SSA, m ² /g	C	Correlation coefficient		Thickness equation	Micropore volume, mm ³ /g	Micropore area, m ² /g	Correlation coefficient
UiO-66@SiO ₂ 1h	40.0	457.2	0.99969	55.466	Harkins and Jura	8.996	22.1	0.993088
UiO-66-NH ₂ @SiO ₂ 1h	133.3	1414.4	0.99996	99.455		38.95	98.3	0.996116

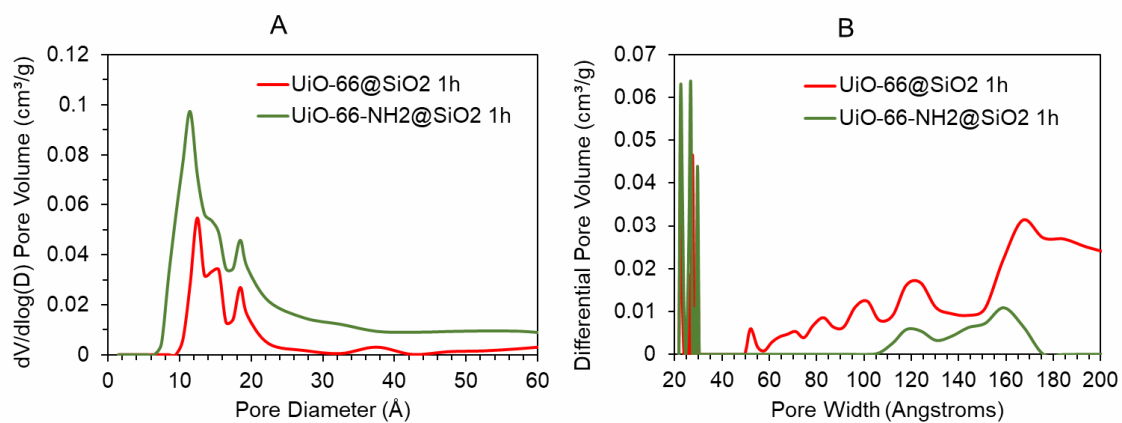


Figure S5. (A) BJH pore size distribution according to adsorption branches of isotherms. (B) Pore size distribution by NLDFT according to the model of cylindrical pores in an oxide surface.

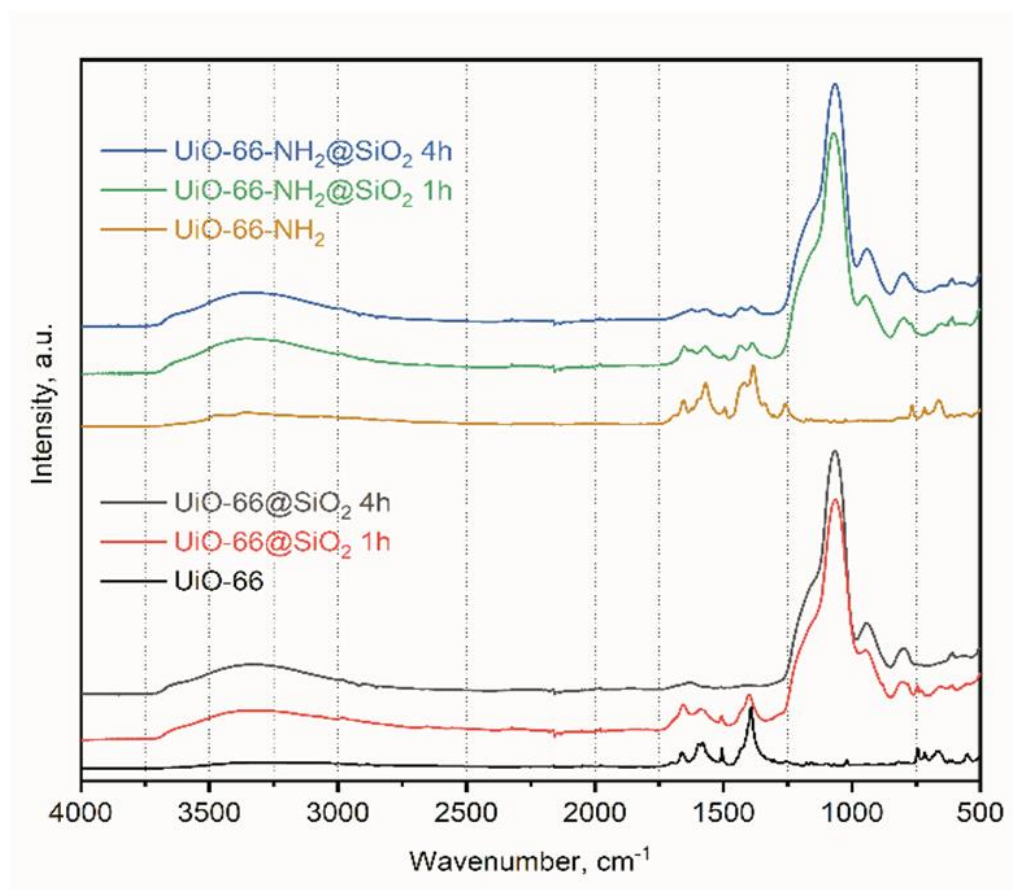


Figure S6. ATR-FTIR spectra collected for intact UiO-66 and UiO-66-NH₂ nanoparticles compared to UiO-66@SiO₂ and UiO-66-NH₂@SiO₂ MOFs treated with TEOS for 1 and 4 h.

PVP grafted UiO-66 in DI water

UiO-66@SiO₂ in DI water

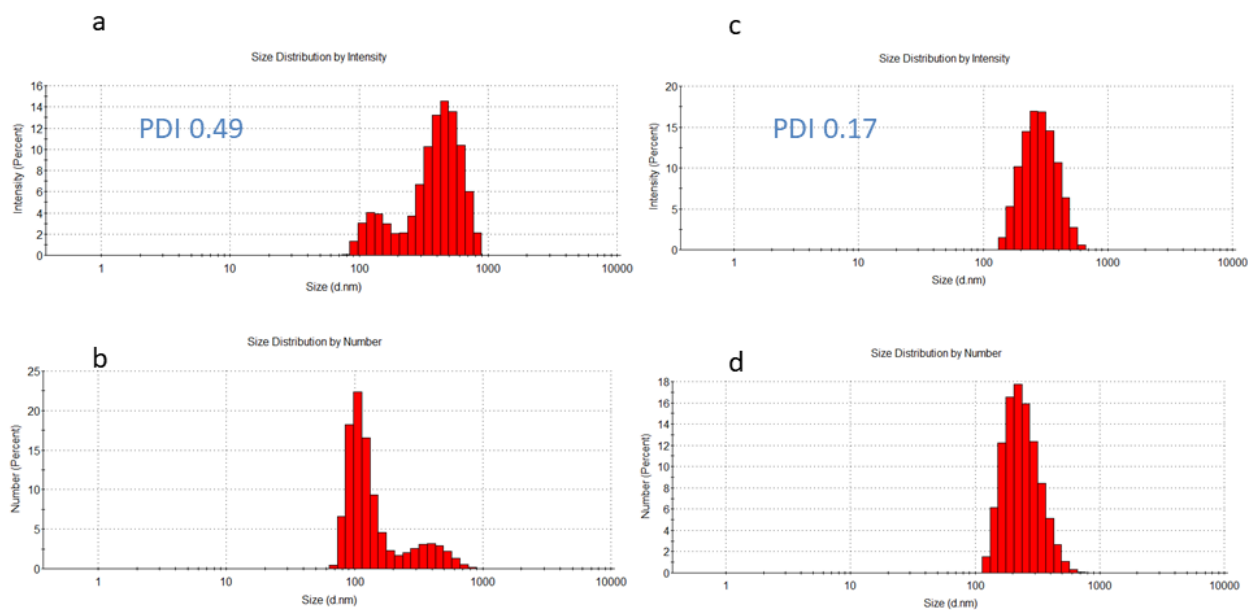


Figure S7. DLS-intensity and DLS-number results for PVP grafted UiO-66 and UiO-66@SiO₂ water dispersions.

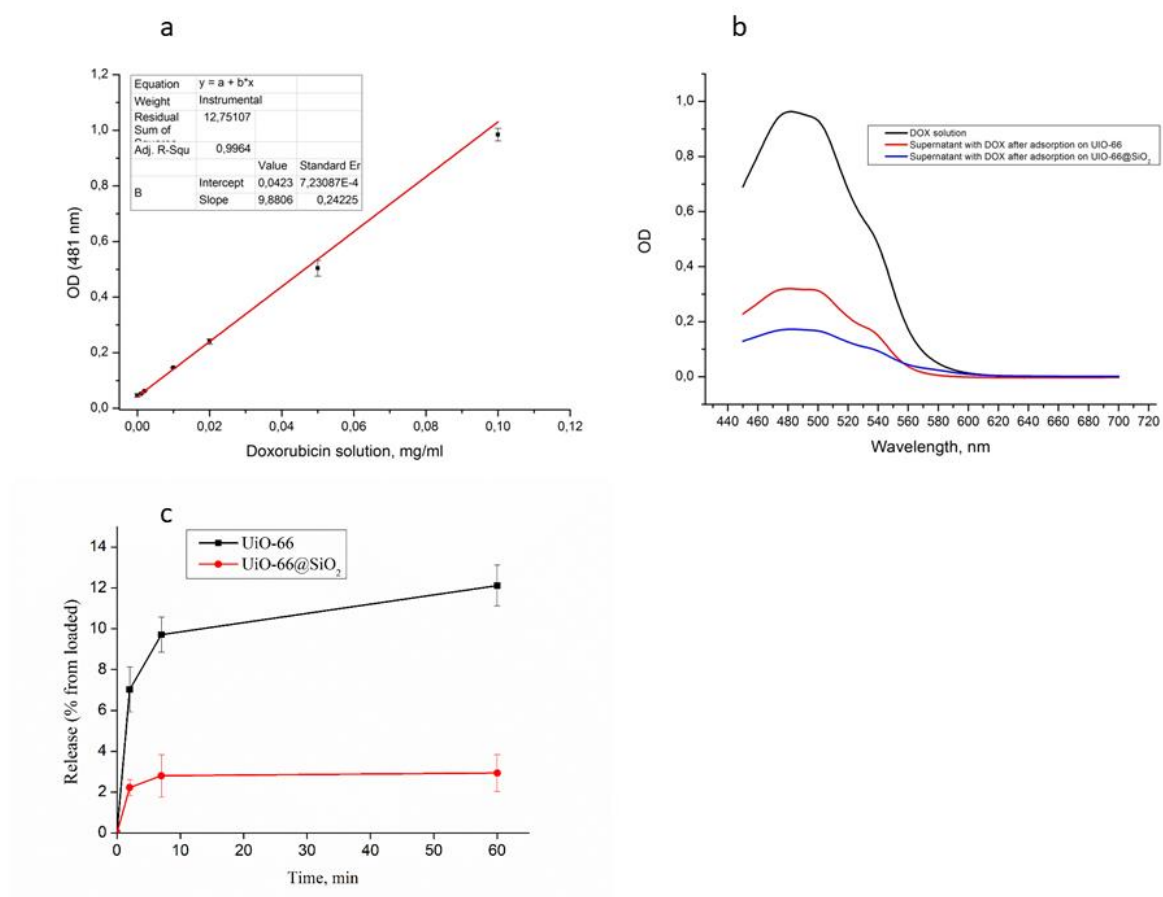


Figure S8. Calibration curve for DOX (a) and absorption spectrum of the DOX solution and DOX in supernatants after loading into MOFs (b), DOX release profiles from UiO-66 and UiO-66@SiO₂ (c) .

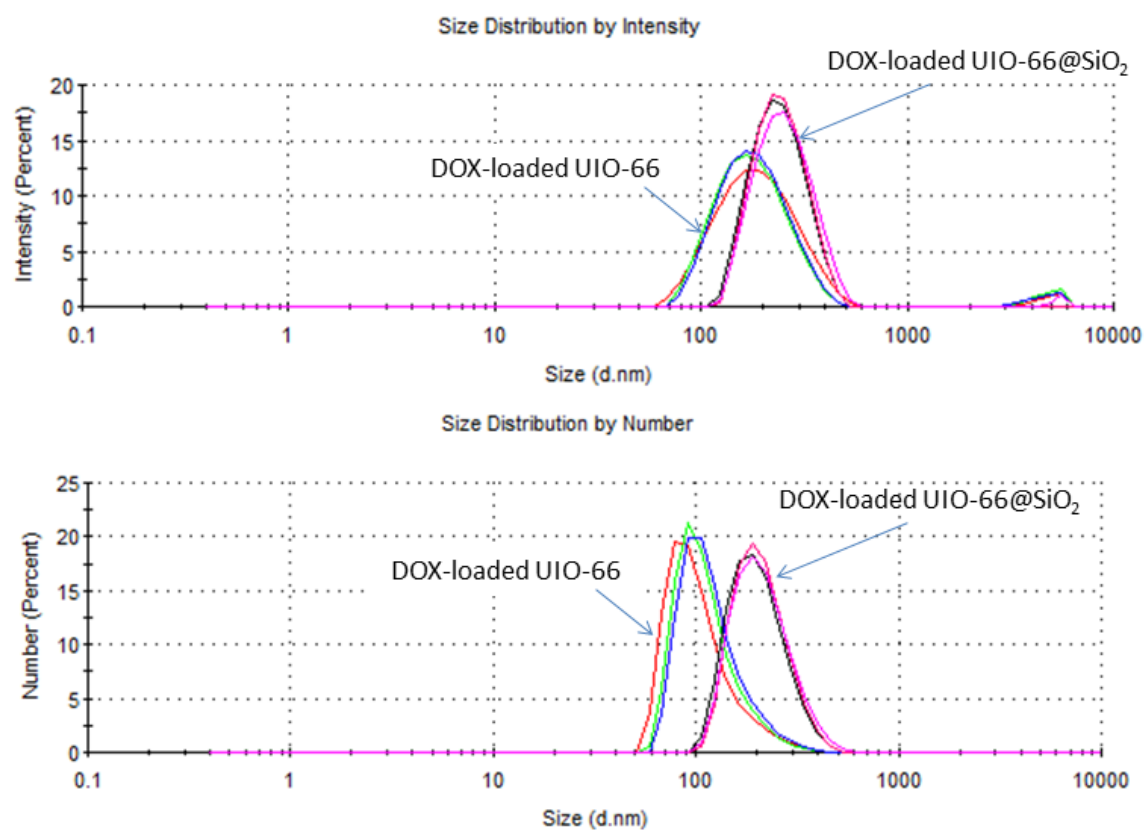


Figure S9. DLS-intensity and DLS-number distributions DOX-loaded UIO-66 and UIO-66@SiO₂.

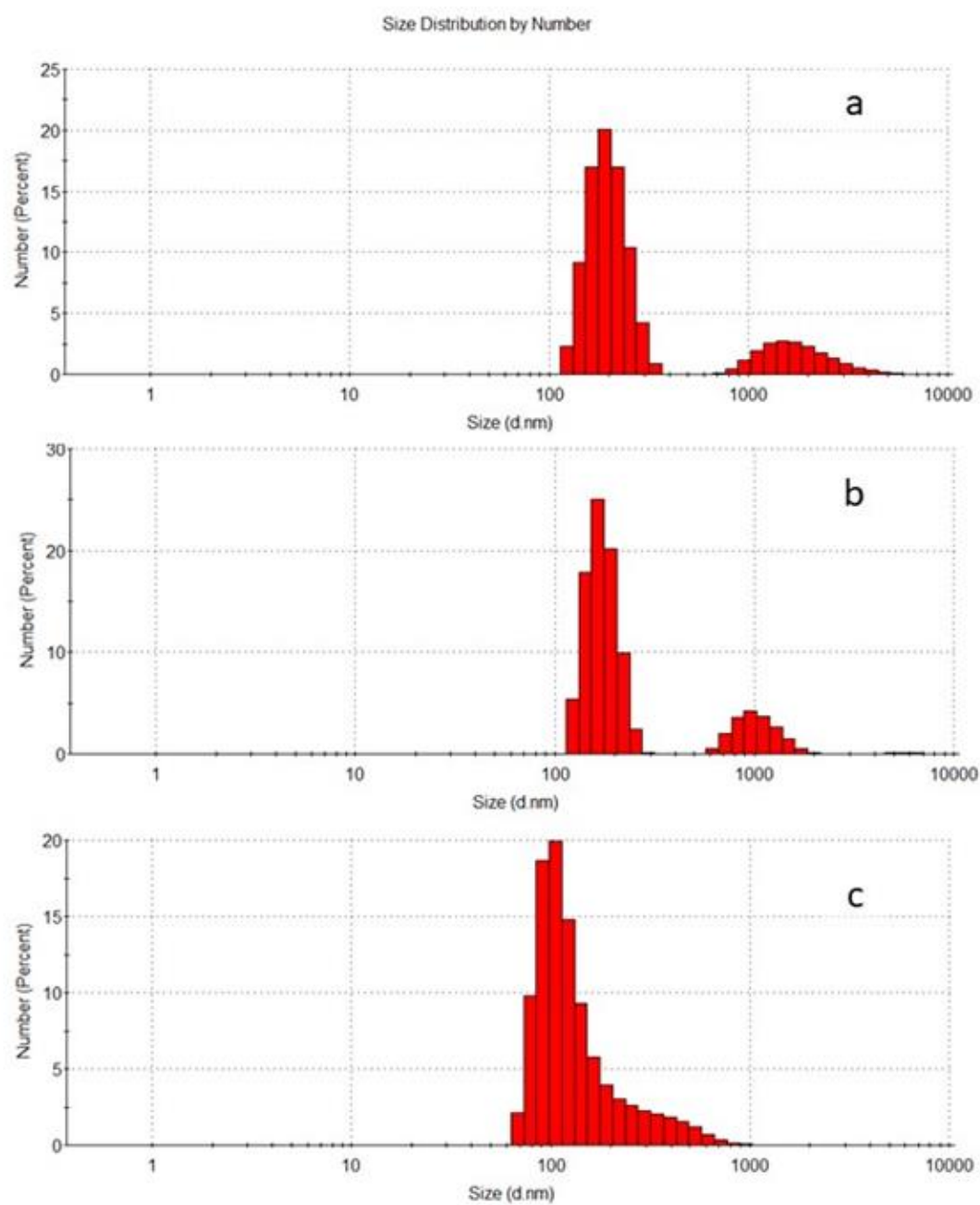


Figure S10. DLS-number distributions of DOX-loaded UiO-66/F127-FA in MEM (a), DMEM (b), RPMI (c) cultural media.